Ultrasensitive Colorimetric DNA Detection using a Combination of Rolling Circle Amplification and Nicking Endonuclease-Assisted Nanoparticle Amplification (NEANA)

*Wei Xu, Xiaoji Xie, Dawei Li, Zhaoqi Yang, Tianhu Li, and Xiaogang Liu**

The rapid growth of genomic DNA sequences has prompted strong demand of low-cost, reliable methods for DNA detection at ultralow concentrations.[1] Common detection approaches including microarray,[2] polymerase chain reaction (PCR),[3] Southern blotting,[4] and rolling circle amplification (RCA),[5] are generally based on DNA hybridization assays, which utilize a single-stranded oligonucleotide as a probe to recognize a specific nucleotide sequence in a target analyte and subsequently hybridize to the target as part of the detection process. Despite their usefulness, there are many constraints associated with these approaches. Most assays involve tedious covalent functionalization of the target with a fluorescent or radioactive tag.[6] Apart from the need of target pre-modification, these approaches also require stringent purification steps and costly instruments.[7]

Alternatively, gold nanoparticles have shown great promise in DNA assays by virtue of their size-dependent optical and electronic properties.[8] Owing to their high extinction coefficients and strong distance-dependent optical properties, gold nanoparticles have enabled rapid colorimetric strategies for DNA detection.[9,10] We have previously demonstrated that target DNA sequences can be directly visualized with the naked eye using nicking endonuclease-assisted nanoparticle amplification (NEANA).[11] This method allows high-sensitivity (ca. 10 pM) detection of long single-stranded oligonucleotides with single-base mismatch selectivity. Despite the advantage over conventional detection techniques, the NEANA approach has a relatively limited scope for detecting random DNA sequences, because of the requirement of a specific sequence for target DNA to be recognized by the nicking enzyme. Here, we show that a combination of the NEANA approach with RCA through use of a padlock probe overcomes the sequence constraint and enables colorimetric detection of random DNA sequences. As an added benefit, the utilization of RCA improves detection sensitivity down to 1 pM.

In our design, we use a padlock oligonucleotide probe for RCA reactions. This probe has one segment with sequence identical to a linker probe **a′b′** and two target-complementary segments present at opposite ends of the molecule (**Scheme 1**). Upon hybridization to a target sequence in the presence of a DNA ligase, the ends are brought in contact to form a circular oligonucleotide. When added to a mixture of DNA polymerase and deoxynucleotide triphosphates (dNTPs), the circularized probe can serve as an efficient template for RCA reactions. As a result, prolonged single-stranded DNA molecules containing many copies of complementary sequence of the padlock template are synthesized using a short DNA primer.[12] Subsequently, a nicking endonuclease and the linker probe (**a′b′**) are added to initiate the NEANA process. Importantly, the nicking reaction occurs

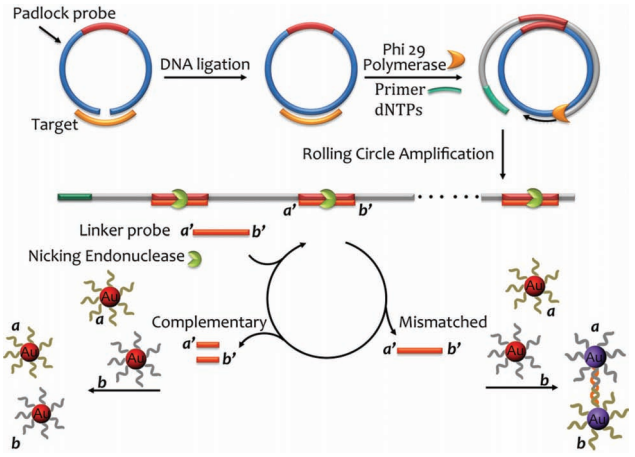

Scheme 1. Colorimetric DNA detection through rolling circle amplification and nicking endonuclease-assisted nanoparticle amplification.

W. Xu, X. Xie, Prof. X. Liu
Department of Chemistry
National University of Singapore
3 Science Drive 3, Singapore 117543
E-mail: chmlx@nus.edu.sg
D. Li, Z. Yang, Prof. T. Li
Division of Chemistry & Biological Chemistry
School of Physical & Mathematical Sciences
Nanyang Technological University
Singapore 637371
Prof. X. Liu
Institute of Materials Research and Engineering
3, Research Link, Singapore 117602

DOI: 10.1002/smll.201200263

 © 2012 Wiley-VCH Verlag GmbH & Co. KGaA, Weinheim

small

simultaneously at many sites along the linear single-stranded DNA products resulting from the RCA process. Upon completion of the strand-scission, two sets of different oligonucleotide-modified gold nanoparticles (probes **a** and **b**) with sequences complementary to that of the linker probe are added to the solution. If the target DNA matches the padlock probe, no aggregation of gold nanoparticles will be observed because of the cleavage of the linker probe through the RCA-coupled NEANA process. Conversely, when the target DNA is not present, no circularized padlock probes and RCA products are formed. Thus, we would observe a color change due to particle aggregation through hybridization of the particle probes and the uncleaved linker probe.

Notably, the end segments of the padlock probe can be easily modified for detecting a specific DNA target sequence without modifying the linker probe and gold nanoparticle probes. Thus, with the assistance of RCA, arbitrary DNA sequences at ultralow concentrations can be readily identified using the same set of linker and particle probes in the presence of nicking enzyme.

As a proof-of-concept experiment, we designed a linear 87-mer oligonucleotide as the padlock probe. The end segments were connected by a ligation reaction, forming a circular probe as the template for RCA. The formation of the circular probe was confirmed by analyzing [γ-^{32}P]-labeled reaction products via 20% denaturing polyacrylamide gel electrophoresis (PAGE). This analysis is based on the fact that oligonucleotides of different sizes and geometries travel at different rates, with linear structures passing more easily than circular structures through the pores in the gel.[13] As shown in **Figure 1** (lane 2), the PAGE analysis of a successful ligation reaction showed two separate bands with a sizable gap between them. By comparison, our control experiment

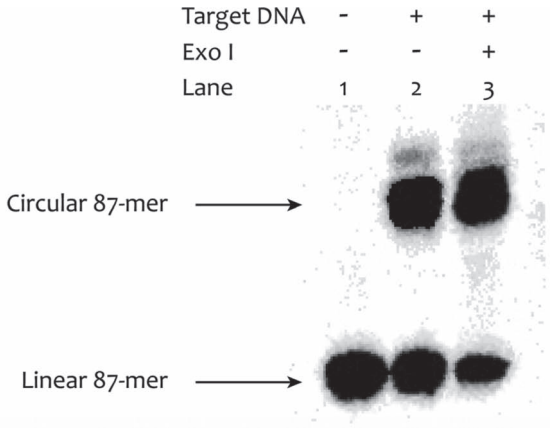

T1: 5'-GCA TCG ACC TGA GAT TTT CCT GCT GGG CAT TCA C-3'
Padlock: 5'-AAA TCT CAG GTC GAT CGA *GCA GGA TGC AGG TGA GGA TCA* TTA CGT aaa gga tcg aat aag agg tcc ttc ACA GAA TGC CCA GCA GGA-3'

Figure 1. Padlock probe circularization analysis through polyacrylamide gel electrophoresis. Lane 1 (control): autoradiogram of polyacrylamide gel separated linear padlock probe with no target added. Lane 2: padlock probe circularization catalyzed by *E. coli.* ligase in the presence of target DNA (**T1**). Lane 3 (control): padlock probe digestion by addition of Exonuclease I (Exo I).

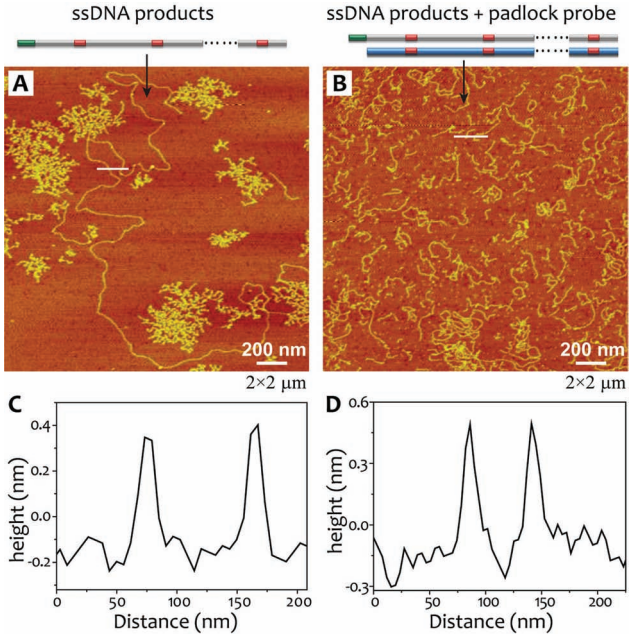

Figure 2. AFM characterization of the RCA products. A) Topographic AFM image of single-stranded DNA (ssDNA) products formed on mica with length up to several micrometers. B) Topographic AFM image of the RCA product hybridized to the padlock probe. C,D) Corresponding height profiles of the DNA products marked in (A) and (B).

without the added target DNA showed only a single band ascribed to the linear 87-mer (Figure 1, lane 1). This result clearly reveals the essential role of target DNA in the process of padlock probe circularization. By analyzing the volume of each band in lane 2, we found that under our experimental conditions (10 units of *E. coli.* DNA Ligase incubated for 2 h) approximately 60% of linear probes were circularized. The circular nature of newly formed oligonucleotides was further confirmed through examination of their resistance to hydrolysis by Exonuclease I.[14] Exonuclease I digests nucleotides one at a time from the end of a linear DNA in a 3′-to-5′ direction, but does not cleave double-stranded or circular DNA.[15] As anticipated, upon addition of Exonuclease I to the reaction mixture after ligation a significant portion of linear probes was digested as evidenced by a markedly diminished band intensity in the gel (Figure 1, lane 3). In contrast, the band intensity of circular probes remained essentially intact.

We subsequently evaluated the feasibility of using as-prepared circular probes for RCA. A primer (5′-TGA TCC TCA CCT GCA TCC T-3′; 1 pmol) was first added to the ligation product (20 μL) and amplified using phi29 polymerase (10 units). After purification, the RCA reaction products were added onto a mica substrate and characterized by atomic force microscopy (AFM). A typical tapping-mode AFM image revealed the presence of single-stranded linear DNA molecules up to a few micrometers long (**Figure 2**A). The DNA molecules on mica have compact structures with lumps and super twisting, largely due to the loop flexibility and intrastrand base-pairing in single-stranded DNA molecules. To provide a better view of the RCA products, the single-stranded DNA products obtained from RCA were

© 2012 Wiley-VCH Verlag GmbH & Co. KGaA, Weinheim

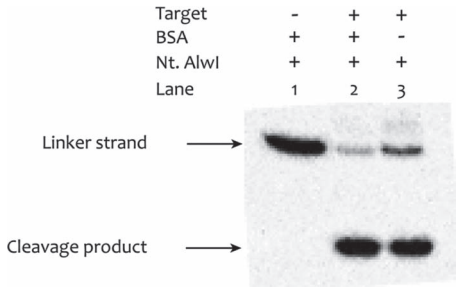

Figure 3. Polyacrylamide gel electrophoretic analysis of oligonucleotide cleavage assays by addition of nicking endonuclease. Lane 1: ^{32}P-labeled 5′ phosphorylated linker strand alone. Lane 2: cleavage of the linker probe using RCA product as the template. Note that BSA was added in both ligation and RCA steps. Lane 3: a control reaction under standard conditions, but without BSA.

further hybridized with complementary padlock probes to form double-stranded DNA molecules. The resulting nicks were closed by ligation before deposition of the molecules onto the mica substrate. AFM image of the double-stranded DNA molecules showed elongated structures owing to the rigidity imposed by the DNA duplexes (Figure 2B). Despite the compact structure of the DNA molecule on mica, it was possible to estimate its height in the loops. The height for single- and double-stranded DNA molecules was measured to be around 0.4 and 0.6 nm, respectively. Taken together, these results clearly demonstrate the successful generation of single-stranded DNA molecules, typically a thousand bases long, from a starting template with only 87 bases (~30 nm).

In a further set of experiments, we validated the cleavage of the linker probe (**a′b′**) by nicking endonuclease through use of RCA product as the template. Using [γ-^{32}P]-labeled linker strands for PAGE analysis, we found that under our experimental conditions (10 units of Nt. AlwI (nicking endonucleases), 10 mM Tris-HCl pH 7.4 (Tris = 2-amino-2-hydroxymethyl-propane-1,3-diol), 10 mM $MgCl_2$, 50 mM NaCl, 1 mM dithiothreitol (DTT), 60 °C, 2 h), the nicking enzyme cleaved more than 82% of linker strands within 2 h (**Figure 3**, lane 3). By comparison, without the added target no cleavage product was observed (Figure 3, lane 1). It should be noted that commonly used bovine serum albumin (BSA) was not added in buffer solutions as the small protein could prevent gold nanoparticles from aggregation and potentially result in a false positive signal readout.[16] Importantly, the absence of BSA (Figure 3, lane 3) did not have a marked affect on the enzymatic reaction as compared to the assay with the BSA (Figure 3, lane 2).

We next tested the colorimetric detection of DNA by RCA-coupled NEANA approach with two different sets of 15-base DNA-modified gold nanoparticles (probes **a** and **b**). We observed that no apparent particle aggregation formed for all solution samples containing target DNA strands at different concentrations (**Figure 4**A), indicating the efficient cleavage of linker strands by the nicking enzyme through repeated RCA product-templated strand-scission cycles. In contrast, precipitation of the gold nanoparticles was clearly seen in the absence of target DNA (Figure 4A). Under our

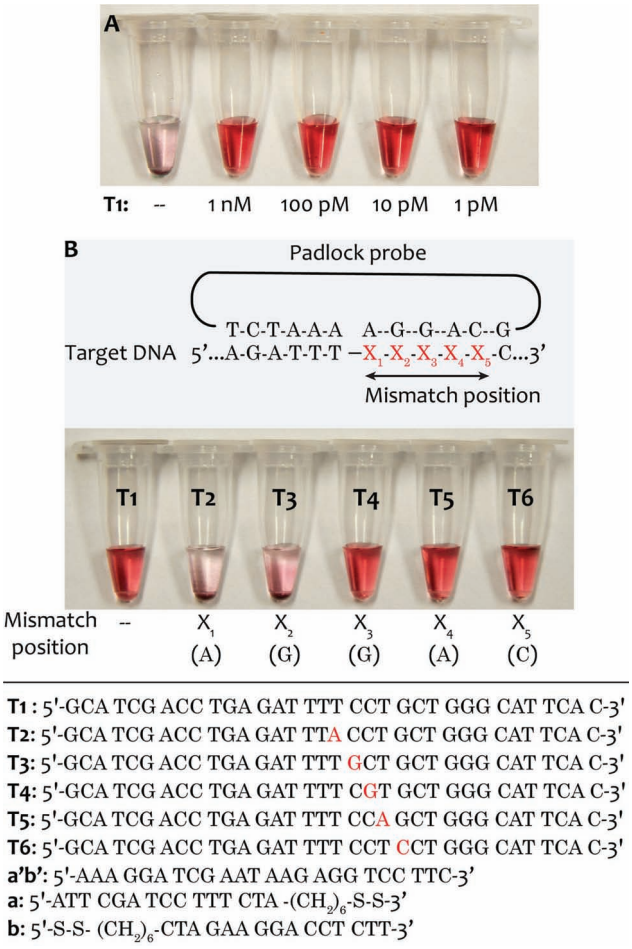

Figure 4. Sensitivity and selectivity assays for DNA detection via the RCA-coupled NEANA approach. A) Photograph showing colorimetric detection of target DNA (**T1**) at various concentrations (1 nM, 100 pM, 10 pM, and 1 pM). B) Photography showing colorimetric response of colloidal solutions to perfectly matched (**T1**; 10 pM) and single-mismatched sequences (**T2** to **T6**; 10 pM each). Mismatched positions are marked with **X1** to **X5**.

standard conditions, this method has a remarkably low detection limit of 1 pM.

To obtain a mechanistic insight into the selectivity of this detection system, we undertook a series of studies that evaluate sequence-dependent ligation efficiency in the padlock circularization step. We found that target sequences were recognized with very high specificity, adequate to detect single-base mismatches in DNA, due to the stringent requirement for hybridization to two target segments at the nick site.[17] In our assays, polymorphic targets were made by introducing single-base mutation at different positions (labeled as **X1** to **X5**) adjacent to the ligation site (Figure 4B). The results for a perfectly matched and five mismatched target DNAs were colorimetrically compared using the RCA-coupled NEANA approach. As shown in Figure 4B, strong position dependent effects of sequence mismatches in target DNA on the ligation reaction are evident. If the mutations are located near the nick site ($\mathbf{X}_1$ and $\mathbf{X}_2$), ligation is significantly hampered, causing the RCA process disrupted. Nanoparticle aggregation occurs as the linker strand added could not be cleaved

© 2012 Wiley-VCH Verlag GmbH & Co. KGaA, Weinheim

small

despite the presence of nicking enzyme. Importantly, in excess of a distance of more than two nucleotide bases from the nick site (e.g., $\mathbf{X}_3$ to $\mathbf{X}_5$), the effect of the mismatched position on the ligation reaction becomes marginalized. As a result, these mismatched sequences cannot be colorimetrically differentiated from a perfectly matched target (Figure 4B).

In conclusion, we have demonstrated the combination of RCA and NEANA for rapid colorimetric DNA detection that eliminates the need for costly and time-consuming target fluorescence-labeling. This technique relies upon high specificity ligation and rolling circle replication of a padlock probe. The coupling of RCA and NEANA provides high sensitivity and great detection capacity for random target sequences by utilizing a fixed set of linker and particle probes and an easily modifiable padlock probe. Furthermore, we expect that this work can be extended for multiplexed colorimetric DNA detection with other types of nanoparticle systems displaying various colors.[9g,18] Applications of the methodology include rapid screening of specific DNA sequences and genotyping of single nucleotide polymorphisms.

Experimental Section

Circularization of the Padlock Probe: A set of 100 µL mixtures containing 10 nM linear padlock probes, various concentrations (1 nM, 100 pM, 10 pM, 1 pM, 0 pM) of the single-stranded target (**T1**), and 1× New England Biolabs (NEB) *E. coli*. Ligase buffer (30 mM Tris-HCl (pH 8.0), 4 mM $MgCl_2$, 26 µM nicotinamide adenine diphosphate (NAD), 1 mM DTT, and 50 µg/mL BSA) was prepared and heated at 95 °C. The vial with target **T1** was used as a control. The ligation reactions were carried out in the presence of *E. coli*. DNA ligase (10 units) for 2 h at 16 °C.

Characterization of Padlock Probe Circularization: The 87-mer linear padlock DNA was first labeled and purified at its 5′-end with [γ-^{32}P] ATP (adenosine triphophate). A mixture of 10 nM ^{32}P-labeled linear padlock probe, 10 nM target DNA, 30 mM Tris-HCl (pH 8.0), 4 mM $MgCl_2$, 26 µM NAD, 1 mM DTT, and 50 µg/mL BSA was then prepared and kept at 95 °C for 5 min, followed by cooling down to 16 °C. After hybridization, *E. coli*. DNA ligase (10 units) was added and the resulting mixture was further incubated at 16 °C for 2 h before being loaded onto a polyacrylamide gel (20% acrylamide).

Exonuclease I Digestion: To confirm the successful formation of circular DNA, [γ-^{32}P]-labeled circularization products were mixed with 67 mM glycine-KOH (pH 9.5), 6.7 mM $MgCl_2$, 10 mM 2-mercaptoethanol, and 10 units of Exonuclease I. The resultant mixture was then incubated at 37 °C for 30 min before being loaded onto a polyacrylamide gel (20% acrylamide).

Rolling Circle Amplification: In a typical experiment, to a 20 µL solution from circularization products were added 10 units of phi29 polymerase, 1 pmol primer, 10 µmol dNTP, 50 mM Tris-HCl (pH 7.5), 10 mM $(NH_4)_2SO_4$, 10 mM $MgCl_2$, and 4 mM DTT, and subsequently incubated for 1 h at 30 °C.

Nicking Endonuclease-Assisted Nanoparticles Amplification: After RCA reaction, 1.5 µL of RCA product was added into a solution containing 3 pmol **a′b′**, 10 mM Tris-HCl (pH 7.4), 50 mM NaCl, 10 mM $MgCl_2$, 1 mM DTT, and 10 units of Nt. AlwI for a nicking reaction at 60 °C for 2 h. After the nicking reaction, two sets of 15-base oligonucleotide-modified gold nanoparticle probes (**a** and **b**, 25 µL each) were added into sample solutions for visual readout of target DNA strands.

Supporting Information

Supporting Information is available from the Wiley Online Library or from the author.

Acknowledgements

This study was supported in part by the Ministry of Education, (MOE2010-T2-083), the Singapore–Peking–Oxford Research, Enterprise (SPORE), and the Singapore–MIT alliance.

[1] J. G. Hacia, L. C. Brody, M. S. Chee, S. P. A. Fodor, F. S. Collins, *Nat. Genet.* **1996**, *14*, 441.

[2] U. Maskos, E. M. Southern, *Nucleic Acids Res.* **1992**, *20*, 1679.

[3] M. Kubista, J. M. Andrade, M. Bengtsson, A. Forootan, J. Jonák, K. Lind, R. Sindelka, R. Sjöback, B. Sjögreen, L. Strömbom, A. Ståhlberg, N. Zoric, *Mol. Aspects Med.* **2006**, *27*, 95.

[4] E. M. Southern, *Trends Biochem. Sci.* **2000**, *25*, 585.

[5] a) P. M. Lizardi, X. Huang, Z. Zhu, P. Bray-Ward, D. C. Thomas, D. C. Ward, *Nat. Genet.* **1998**, *19*, 225; b) J. Li, Y. Chu, Y. Lee, X. Xie, *Nucleic Acids Res.* **2008**, *36*, e36; c) M. M. Ali, Y. Li, *Angew. Chem.Int. Ed.* **2009**, *48*, 3512.

[6] a) J. Schotter, P. B. Kamp, A. Becker, A. Pühler, G. Reiss, H. Brückl, *Biosens. Bioelectron.* **2004**, *19*, 1149; b) X. Zuo, F. Xia, Y. Xiao, K. W. Plaxco, *J. Am. Chem. Soc.* **2010**, *132*, 1816; c) M. M. Ali, S. D. Aguirre, H. Lazim, Y. Li, *Angew. Chem. Int. Ed.* **2011**, *50*, 3751; d) R. Kong, X. Zhang, Z. Chen, H. Meng, Z. Song, W. Tan, G. Shen, R. Yu, *Anal. Chem.* **2011**, *83*, 7603.

[7] a) E. M. Southern, *J. Mol. Biol.* **1975**, *98*, 503; b) H. Zhang, W. Xu, X. Liu, F. Stellacci, J. T. L. Thong, *Appl. Phys. Lett.* **2010**, *97*, 163702.

[8] a) J. Zhang, *J. Phys. Chem. Lett.* **2010**, *1*, 686; b) H. Wei, Z. Wang, J. Zhang, S. House, Y. Gao, L. Yang, H. Robinson, L. H. Tan, H. Xing, C. Hou, I. M. Robertson, J. Zuo, Y. Lu, *Nat. Nanotechnol.* **2011**, *6*, 93; c) P. Chen, D. Pan, C. Fan, J. Chen, K. Huang, D. Wang, H. Zhang, Y. Li, G. Feng, P. Liang, L. He, Y. Shi, *Nat. Nanotechnol.* **2011**, *6*, 639; d) Y. Xiao, K. Y. Dane, T. Uzawa, A. Csordas, J. Qian, H. T. Soh, P. S. Daugherty, E. T. Lagally, A. J. Heeger, K. W. Plaxco, *J. Am. Chem. Soc.* **2010**, *132*, 15299; e) M. M. Ali, P. Kanda, S. D. Aguirre, Y. Li, *Chem. Eur. J.* **2011**, *17*, 2052; f) X. Xie, W. Xu, T. Li, X. Liu, *Small* **2011**, *7*, 1393; g) Y. Song, X. Xu, K. W. MacRenaris, X. Zhang, C. A. Mirkin, T. J. Meade, *Angew. Chem. Int. Ed.* **2009**, *48*, 9143; h) H. Wang, W. Xu, H. Zhang, D. Li, Z. Yang, X. Xie, T. Li, X. Liu, *Small* **2011**, *7*, 1987; i) J. Zhang, L. Wang, H. Zhang, F. Boey, S. Song, C. Fan, *Small* **2010**, *6*, 201; j) A. E. Prigodich, O. S. Lee, W. L. Daniel, D. S. Seferos, G. C. Schatz, C. A. Mirkin, *J. Am. Chem. Soc.* **2010**, *132*, 10638; k) Y. Huang, H. Liu, X. Xiong, Y. Chen, W. Tan, *J. Am. Chem. Soc.* **2009**, *131*, 17328; l) X. Xue, W. Xu, F. Wang, X. Liu, *J. Am. Chem. Soc.* **2009**, *131*, 11668; m) Z. Zhu, C. Wu, H. Liu, Y. Zou, X. Zhang, H. Kang, C. Yang, W. Tan, *Angew. Chem. Int. Ed.* **2010**, *49*, 1052; n) X. Xue, F. Wang, X. Liu, *J. Am. Chem. Soc.* **2008**, *130*, 3244; o) Y. Xiang, Y. Lu, *Nat. Chem.* **2011**, *3*, 697; p) Z. Wang, J. Zhang, J. M. Ekman, P. J. A. Kenis, Y. Lu, *Nano Lett.* **2010**, *10*, 1886; q) R. Liu, R. Liew, J. Zhou, B. Xing, *Angew. Chem. Int. Ed.* **2007**, *46*, 8799.

© 2012 Wiley-VCH Verlag GmbH & Co. KGaA, Weinheim

[9] a) Y. Cao, R. Jin, C. A. Mirkin, *Science* **2002**, *297*, 1536; b) N. L. Rosi, C. A. Mirkin, *Chem. Rev.* **2005**, *105*, 1547; c) J. Liu, Z. Cao, Y. Lu, *Chem. Rev.* **2009**, *109*, 1948; d) D. Li, S. Song, C. Fan, *Acc. Chem. Res.* **2010**, *43*, 631; e) Y. Song, W. Wei, X. Qu, *Adv. Mater.* **2011**, *23*, 4215; f) F. Xia, X. Zuo, R. Yang, Y. Xiao, D. Kang, A. Vallée-Bélisle, X. Gong, J. D. Yuen, B. Y. Hsu, A. J. Heeger, K. W. Plaxco, *Proc. Natl. Acad. Sci. USA* **2010**, *107*, 10837; g) J. Kim, J. Lee, *Nano Lett.* **2009**, *9*, 4564; h) S. Guo, E. Wang, *Acc. Chem. Res.* **2011**, *44*, 491; i) X. Xue, F. Wang, X. Liu, *J. Mater. Chem.* **2011**, *21*, 13107; j) J. Liu, Y. Lu, *J. Am. Chem. Soc.* **2003**, *125*, 6642; k) M. Hong, X. Zhou, Z. Lu, J. Zhu, *Angew. Chem. Int. Ed.* **2009**, *48*, 9503; l) K. Jang, H. Lee, H. Jin, Y. Park, J. Nam, *Small* **2009**, *5*, 2665.

[10] a) E. Tan, J. Wong, D. Nguyen, Y. Zhang, B. Erwin, L. K. van Ness, S. M. Baker, D. J. Galas, A. Niemz, *Anal. Chem.* **2005**, *77*, 7984; b) J. Jian, C. Huang, *Chem. Eur. J.* **2011**, *17*, 2374; c) J. Li, T. Deng, X. Chu, R. Yang, J. Jiang, G. Shen, R. Yu, *Anal. Chem.* **2010**, *82*, 2811; d) L. Cui, G. Ke, W. Zhang, C. Yang, *Biosens. Bioelectron.* **2011**, *26*, 2796; e) J. Zhao, T. Liu, Q. Fan, G. Li, *Chem. Commun.* **2011**, *47*, 5262.

[11] W. Xu, X. Xue, T. Li, H. Zeng, X. Liu, *Angew. Chem. Int. Ed.* **2009**, *48*, 6489.

[12] A. Fire, S. Xu, *Proc. Natl. Acad. Sci. USA* **1995**, *92*, 4641.

[13] Y. Wang, X. Li, X. Liu, T. Li, *Chem Commun.* **2007**, 4369.

[14] T. Zhou, G. Chen, Y. Wang, Q. Zhang, M. Yang, T. Li, *Nucleic Acids Res.* **2004**, *32*, e173.

[15] I. R. Lehman, A. L. Nussbaum, *J. Biol. Chem.* **1964**, *239*, 2628.

[16] a) Y. N. Tan, X. Su, E. Liu, J. S. Thomsen, *Anal. Chem.* **2010**, *82*, 2759; b) N. Yang, X. Su, V. Tjong, W. Knoll, *Biosens. Bioelectron.* **2007**, *22*, 2700.

[17] a) S. M. Panasenko, J. R. Cameron, R. W. Davis, I. R. Lehman, *Science* **1977**, *196*, 188; b) E. Lai, *Genome Res.* **2001**, *11*, 927.

[18] a) H. Park, J. Joo, H. Kim, J. Lee, *J. Phys. Chem. C* **2012**, *116*, 2278; b) S. Han, J. Lee, *Langmuir* **2012**, *28*, 828; c) F. Wang, X. Liu, *J. Am. Chem. Soc.* **2008**, *130*, 5642; d) R. Deng, X. Xie, M. Vendrell, Y. T. Chang, X. Liu, *J. Am. Chem. Soc.* **2011**, *133*, 20168; e) F. Wang, R. Deng, J. Wang, Q. Wang, Y. Han, H. Zhu, X. Chen, X. Liu, *Nat. Mater.* **2011**, *10*, 968.

Received: February 5, 2012
Published online: March 28, 2012

 © 2012 Wiley-VCH Verlag GmbH & Co. KGaA, Weinheim